DEVELOPMENT AND CHARACTERIZATION OF A LOW-FREQUENCY NOISE MEASUREMENT SYSTEM FOR OPTOELECTRONIC DEVICES

Marko Jankovec, Marko Topič

Faculty of Electrical Engineering, University of Ljubljana, Ljubljana, Slovenia

Key words: noise measurement, FFT spectrum analyzer, transconductance amplifier, 1/*f* noise

Abstract: A noise spectral density measurement system for low-frequency current noise was built and thoroughly characterized from dynamic and noise point of view. The system uses the SR570 transconductance amplifier and the SR780 FFT spectrum analyzer. The built in battery power supply in the SR570 together with an effective double shielding arrangement enables good low frequency interference protection in noisy environments. Results of dynamic and noise analyses and a resulting comprehensive noise model of the SR570 are presented. Besides other noise parameters also 1/*f* noise components of noise sources in the SR570 are identified. Further, the influence of DUT impedance to the overall system noise properties is shown. The noise measurement system performance utilizing the developed noise model is demonstrated by the low-frequency noise measurement of a-Si:H *pin* diode.

Razvoj in karakterizacija nizkofrekvenčnega šumnega merilnega sistema za optoelektronske elemente

Kjučne besede: šumne meritve, FFT spektralni analizator, transkonduktančni ojačevalnik, 1/*f* šum

Izvleček: Zgradili smo šumni merilni sistem za meritev gostote močnostnega spektra tokovnega šuma pri nizkih frekvencah in ga natančno okarakterizirali iz dinamičnega in šumnega vidika. V merilnem sistemu sta uporabljena transkonduktančni ojačevalnik SR570 in FFT spektralni analizator SR780. Vgra-jeno baterijsko napajanje v SR570 skupaj z učinkovitim dvojnim oklopom omogoča visoko odpornost proti nizkofrekvenčnim motnjam v šumnem laboratorijskem okolju. V članku predstavljamo rezultate dinamične in šumne analize merilnega sistema ter celotnega šumnega modela ojačevalnika SR570. Poleg kataloških šumnih parametrov smo ovrednotili tudi 1/*f* spektralne komponente šumnih virov ojačevalnika SR570. Nadalje je pokazan vpliv impedance merjenca na šumne lastnosti celotnega merilnega sistema. Delovanje šumnega merilnega sistema in uporabo šumnega modela smo prikazali na primeru meritve nizkofrekvenčnega šuma a-Si:H *pin* diode.

1. Introduction

Noise performance of any kind of photodetection system is basically determined by noise of photodetector and noise of readout electronics /1/. The upper limit of signal-to-noise ratio and dynamic range of the whole system are initially determined by the noise of the detector. In the case of a photodiode, the useful signal is usually superimposed by a random component, which is a consequence of concentration and mobility fluctuations of free charge carriers. This random signal can be expressed as a superposition of shot, 1/*f* (flicker) and thermal noise sources /2/. While the physical backgrounds of thermal and shot noise are well known, the origin of 1/*f* noise is still a matter of research /3/.

If a photodetector operates in a charge storage mode, when its (DC) current signal is integrated in a storage capacitance and read out after certain integration time, the 1/*f* noise becomes important /4/. Additionally, the 1/*f* noise investigation of low-quality material devices, such as a-Si:H TFTs or *pin* diodes, gives deeper insight into the device physics providing potential for improvements /5, 6/. Since the 1/*f* noise of a photodetector is an important parameter, especially at low radiation intensities and high speed readout requirements, its quantitative determination is necessary for device characterization and optimization of the readout electronics.

We have built-up a low frequency current noise spectral density measurement setup for two-terminal devices, which is mainly intended for low-frequency noise spectral density measurements of optoelectronic detectors. Prior to any device characterization a comprehensive test of the measurement setup was performed since various internal and external noise sources contribute to the total system noise and have to be evaluated and separated from the signal that originates from the Device Under Test (DUT). Furthermore, the influence of the impedance of the DUT to the noise properties of the measurement system was investigated. Finally, the obtained noise model of the measurement system was applied for noise measurement of an α-Si:H *pin* diode.

2. Measurement system

The noise measurement setup is presented in fig. 1. It consists of a double shielded measurement box, a battery powered Low-Noise Amplifier (LNA) and a Fast-Fourier Transform (FFT) spectrum analyzer. Temperature of the

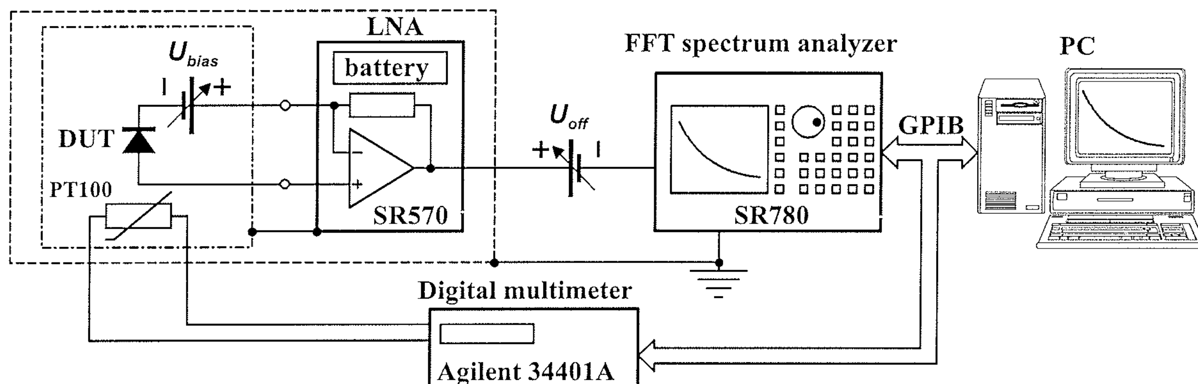

Fig. 1: Noise measurement setup with variable voltage bias (U_{bias}) and offset (U_{off}) sources, temperature monitoring and double shielding from external interference.

inner measurement box is monitored by a PT100 temperature sensor, whose resistance is acquired by an Agilent 34401A digital multimeter. Both digital instruments are controlled by personal computer (PC) via General Purpose Instrument Bus (GPIB).

Conventional spectrum analyzers which are based on a heterodyne principle have limited lower frequency range (arround 10 Hz) making them less suitable for 1/*f* noise measurement. On the contrary, FFT spectrum analyzers have fundamental upper frequency limit due to limited calculation capabilities, while their lower frequency limit is only determined by the available measurement time, since they can sample the signal over arbitrarily long period and perform the FFT transform to calculate the spectral density. For our system we chose the SR780 FFT spectrum analyzer made by Stanford Research System /7/. It features a wide range of frequency spans from 102.4 kHz down to 195.3 mHz with maximum resolution of 800 points thus enabling noise spectral density measurements resolution up to 244 mHz. Further, the built in 18-bit A/D converter together with low noise input amplifier stage offers high dynamic range useful for measuring low amplitude signal superimposed to higher DC bias.

The choice of LNA as a critical system component depends on the expected type of DUTs and the desired measurement quantities. Since the output of a photodetector is usually a current signal, we looked for a transconductance amplifier for current noise measurements. For its proper operation, the transconductance has to be lower than the DUT admittance, which might be a problem in the case of low resistive or high capacitive DUTs, due to input voltage noise amplification. Considering all these facts we chose SR570 /8/ as the most appropriate LNA. It features low input current and voltage noise, and its transconductance can be set from 1 mA/V down to 1 pA/V, where it uses one of two different input preamplifiers, each for its own sensitivity range. For extremely low signal measurements, the built in lead-acid rechargeable batteries for off-line powering minimize power-line interference noise problems. External interference with the connections of DUT and bias source at the input of the SR570 is suppressed by a careful coaxial cabling, which is additionally reduced by a high-permeability mumetal box. The mumetal box is together with the SR570 enclosed in a bigger aluminum box.

Although the SR570 is equipped with current offset and voltage bias sources that can be useful in some cases, it turned out that they generate too much additional noise to be useful for our design rules. Thus, we had to introduce two external variable voltage sources U_{bias} and U_{off} (Fig. 1) for biasing DUTs and for canceling a consecutive output voltage offset, respectively. Both are made of a sealed lead-acid battery and a variable wire wound resistor divider, which features the lowest intrinsic noise. The equivalent resistance of divider is approximately 500 Ω with negligible effect to the noise of the whole system. The chosen battery capacity is high enough to sustain a fixed DC voltage for 12 hours. All noise measurements were taken at room temperature in an air-conditioned room with well defined temperature stabilization (25 ± 0.5 °C).

3. Results

Prior to noise measurement of any DUT a detailed characterization of the measurement system has to be performed. Due to wide dynamic range of the SR780, the overall noise of the measurement system is determined solely by the LNA, which will be investigated further in detail. The simplified scheme of the transconductance amplifier SR570 is presented in fig. 2.

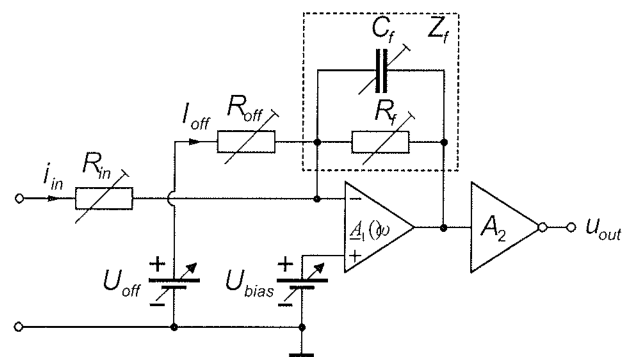

Fig. 2: The simplified scheme of a transconductance amplifier SR570.

It basically consists of an ultra low-noise operational amplifier with feedback resistance R_f. The value R_f is equal to the inverse value of the transconductance down to 100 pA/V for decade values, while below 100 pA/V the sensitivity is increased by a second stage voltage amplifier A_2. Although not desired in some cases, the added variable feedback capacitance can lower the bandwidth of preamplifier to compensate the voltage noise enhancement in the case of high capacitive input termination. For that reason an input resistance R_{in} is included, which is set according to the value of R_f in order to limit the voltage gain of the amplifier in the case of low impedance of the DUT.

3.1. Small signal model of SR570

Fig. 3 presents the small signal model of the amplifier. The feedback impedance $\underline{Z}_f$ (C_f | | R_f) is transformed to the input as a Miller impedance $\underline{Z}_{fmil}$ according to the open loop gain of the front stage $\underline{A}_1(\omega)$, which is modeled as a DC gain A_0 with two poles ω_1 and ω_2. For the second stage a constant voltage gain A_2 in the investigated frequency range is assumed. Thus the voltage drop on $\underline{Z}_{fmil}$ caused by the input current $\underline{I}_{in}$ is amplified by both gain stages $\underline{A}_1(\omega)$ and A_2 (Eq. 3).

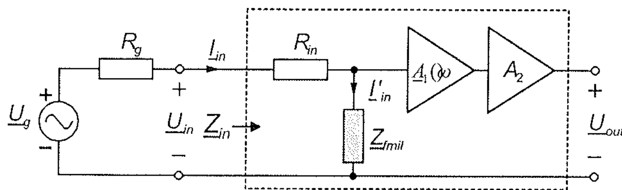

Fig. 3: The small signal model of the SR570 amplifier.

$$\underline{A}_1(\omega) = \frac{A_0}{(1 + j\,\omega/\omega_1)(1 + j\,\omega/\omega_2)} \tag{1}$$

$$\underline{Z}_{fmil}(\omega) = \frac{\underline{Z}_f}{1 + \underline{A}_1} = \frac{1}{1 + \underline{A}_1}\left(\frac{R_f}{1 + j\omega R_f C_f}\right) \tag{2}$$

$$\underline{U}_{out}(\omega) = \underline{A}_1 A_2 \underline{Z}_{fmil} \cdot \underline{I}_{in} \tag{3}$$

In order to determine small signal parameters of the amplifier, the internal and external transfer characteristics from DC to 100 kHz have been measured.

$$\underline{H}(\omega) = \frac{\underline{U}_{out}}{\underline{U}_{in}} = \underline{A}_1 A_2 \frac{\underline{Z}_{fmil}}{R_{in} + \underline{Z}_{fmil}}, \tag{4}$$

$$\underline{H}_{ext}(\omega) = \frac{\underline{U}_{out}}{\underline{U}_g} = \underline{A}_1 A_2 \frac{\underline{Z}_{fmil}}{R_g + R_{in} + \underline{Z}_{fmil}}. \tag{5}$$

By comparing the dynamic model output to the measured data (fig. 4 and fig. 5), we have obtained small signal parameters of the model, which are listed in table 1. The experimentally determined values are denoted in bold, all other are taken from the SR570 datasheet. The differences in A_0 and ω_1 values are due to the usage of two different input preamplifiers.

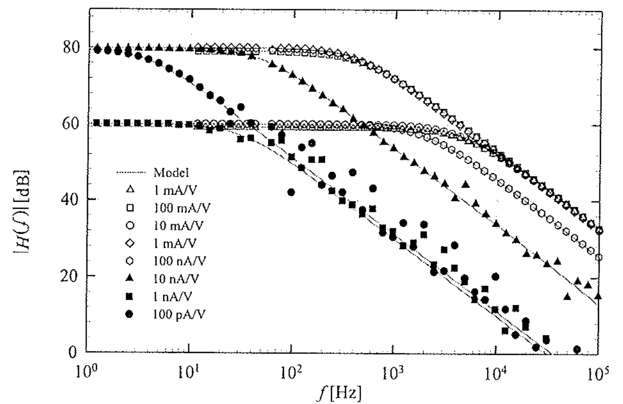

Fig. 4: Measured frequency characteristics of the SR570 voltage gain (symbols) at different sensitivities, compared with the small signal model results (lines).

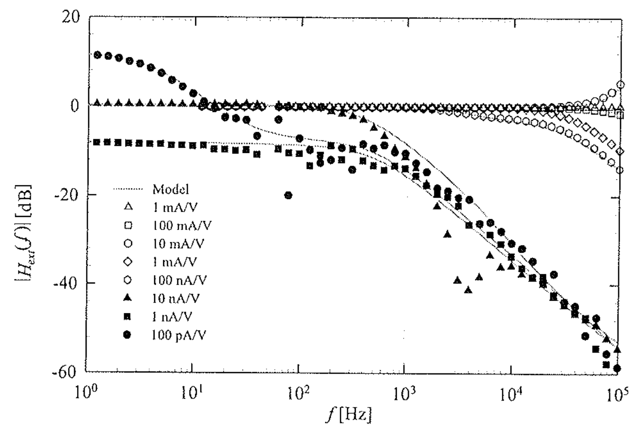

Fig. 5: Measured frequency characteristics of the SR570 external voltage gain (symbols) at different sensitivities, compared with the small signal model results (lines).

Table 1: Parameters of the SR570 small signal model at different transconductance settings.

Transconductance [A/V]	R_g [Ω]	R_f [Ω]	R_{in} [Ω]	B_{-3dB} [Hz]	C_f [pF]	A_0 [V/V]	$\omega_1/2\pi$ [Hz]	$\omega_2/2\pi$ [Hz]
10^{-3}	10^3	10^3	1	$1\cdot10^6$	**110**	**$4\cdot10^6$**	**1.10**	**$2\cdot10^5$**
10^{-4}	10^4	10^4	1	$5\cdot10^5$	**110**	**$4\cdot10^6$**	**1.10**	**$2\cdot10^5$**
10^{-5}	10^5	10^5	100	$2\cdot10^5$	**6.0**	**$4\cdot10^6$**	**1.10**	**$2\cdot10^5$**
10^{-6}	10^6	10^6	100	$2\cdot10^4$	**6.0**	**$4\cdot10^6$**	**1.10**	**$2\cdot10^5$**
10^{-7}	10^7	10^7	10^4	$2\cdot10^3$	**4.8**	**$4\cdot10^6$**	**1.10**	**$2\cdot10^5$**
10^{-8}	$9.6\cdot10^7$	10^8	10^4	200	**4.2**	**10^6**	**0.55**	**$2\cdot10^5$**
10^{-9}	$2.6\cdot10^9$	10^9	10^6	15	**4.2**	**10^6**	**0.55**	**$2\cdot10^5$**
10^{-10}	$2.6\cdot10^9$	10^{10}	10^6	10	**4.2**	**10^6**	**0.55**	**$2\cdot10^5$**
10^{-11}	$2.6\cdot10^9$	10^{11}	10^6	10	**4.2**	**10^6**	**0.55**	**$2\cdot10^5$**
10^{-12}	$2.6\cdot10^9$	10^{12}	10^6	10	**4.2**	**10^6**	**0.55**	**$2\cdot10^5$**

3.2. Noise model of SR570

The noise model of the SR570 is shown in fig. 6 (dashed box) together with the noise model of the DUT.

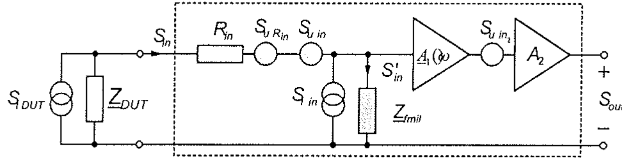

Fig. 6: The SR570 noise model with the DUT's impedance (Z_{DUT}) and current noise source ($S_{i DUT}$).

The DUT model is represented by the impedance Z_{DUT} and a current noise source $S_{i DUT}$. In the SR570 small signal model additional current and voltage noise sources are added, where only the voltage noise source $S_{u R_{in}}$, which represents the thermal noise of the input resistance R_{in}, can be analytically expressed:

$$S_{u R_{in}} = 4kTR_{in}. \quad (6)$$

Other noise sources (equivalent input voltage and current noise sources $S_{u in}$ and $S_{i in}$ and input voltage noise of the second stage $S_{u in2}$) can only be determined by the noise measurement of the amplifier at certain input conditions, at which only one of the noise sources prevails over others. The output noise S_{out} is a consequence of all noise sources

$$S_{out}(\omega) = \left(S'_{in}(\omega)\left|\underline{Z}_{fmil}\underline{A}_1\right|^2 + S_{u in_2}\right)A_2^2, \quad (7)$$

where the equivalent input noise S'_{in} can be expressed as:

$$S'_{in}(\omega) = \frac{S_{i in}(\omega)\cdot\left|\underline{Z}_{DUT} + R_{in}\right|^2 + S_{i DUT}(\omega)\cdot\left|\underline{Z}_{DUT}\right|^2 + S_{u in}(\omega) + S_{u R_{in}}}{\left|\underline{Z}_{DUT} + R_{in} + \underline{Z}_{fmil}\right|^2}. \quad (8)$$

At open circuit input conditions $\left|\underline{Z}_{DUT}\right| \to \infty$ we can assume

$$S_{i DUT}(\omega) \to 0 \;\Rightarrow\; S'_{in}(\omega) = S_{i in}(\omega), \quad (9)$$

and consequently becomes

$$S_{out}(\omega) = \left(S_{i in}(\omega)\left|\underline{Z}_{fmil}\underline{A}_1\right|^2 + S_{u in_2}\right)A_2^2. \quad (10)$$

The output noise can be transferred to the input

$$S_{in}(\omega) = S_{i in}(\omega) + \frac{S_{u in_2}}{\left|\underline{Z}_{fmil}\underline{A}_1\right|^2} \approx S_{i in}(\omega) + \frac{S_{u in_2}}{\left|\underline{Z}_f\right|^2}, \quad (11)$$

where at lower frequencies the input current noise $S_{i in}$ dominates, while towards higher frequencies the second stage voltage noise prevails due to drop of feedback impedance Z_f. In fig. 7 the measured and calculated current noise density spectra transferred to the input at open circuit input conditions of SR570 are presented, from which the parameters of the equivalent input current noise source $S_{i in}$ and second stage voltage noise source $S_{u in2}$ are determined. The input noise current source is described as a sum of flat spectrum and $1/f$ component in a form of .

$$S = S_0 + A_f / f^{\gamma} \quad (12)$$

The square roots values of parameters S_0, A_f, γ and $S_{u in2}$ at different transconductance settings are listed in table 2.

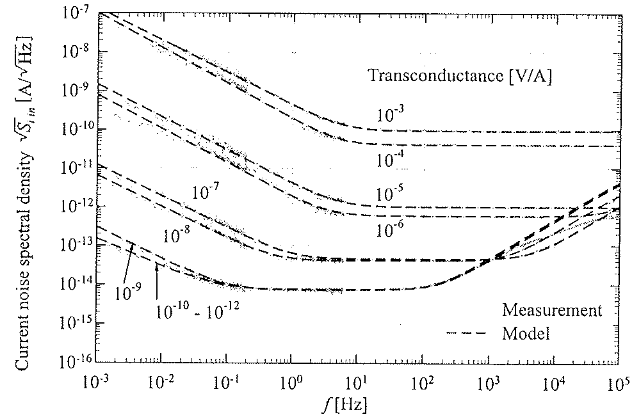

Fig. 7: Measured (full line) and calculated (dashed line) current noise density spectra of the SR570 transferred to the input at open circuit conditions.

Table 2: The list of parameters of the equivalent input current noise source $S_{i in}$ and second stage voltage noise source $S_{u in2}$.

	$S_{i in} = S_0 + A_f / f^{\gamma}$			$S_{u in_2}$
Transconductance [A/V]	$\sqrt{S_0}$ [A/√Hz]	$\sqrt{A_f}$ [A/√Hz]	γ	$\sqrt{S_{u in_2}}$ [V/√Hz]
10^{-3}	$9.3\cdot10^{-11}$	$4.3\cdot10^{-10}$	1.66	0
10^{-4}	$4.1\cdot10^{-11}$	$1.9\cdot10^{-10}$	1.82	0
10^{-5}	$9.9\cdot10^{-13}$	$4.2\cdot10^{-12}$	1.70	0
10^{-6}	$5.4\cdot10^{-13}$	$1.8\cdot10^{-12}$	1.76	$2.2\cdot10^{-7}$
10^{-7}	$4.0\cdot10^{-14}$	$4.4\cdot10^{-14}$	1.64	$3.2\cdot10^{-7}$
10^{-8}	$3.0\cdot10^{-14}$	$2.3\cdot10^{-14}$	1.64	$8.4\cdot10^{-7}$
10^{-9}	$7.1\cdot10^{-15}$	$1.1\cdot10^{-15}$	1.64	$1.7\cdot10^{-6}$
10^{-10}	$7.5\cdot10^{-15}$	$1.1\cdot10^{-15}$	1.44	$1.7\cdot10^{-6}$
10^{-11}	$7.5\cdot10^{-15}$	$1.1\cdot10^{-15}$	1.44	$1.7\cdot10^{-6}$
10^{-12}	$7.5\cdot10^{-15}$	$1.1\cdot10^{-15}$	1.44	$1.7\cdot10^{-6}$

The remaining noise parameter of SR570 that has to be determined is equivalent input voltage noise $S_{u in}$, which can be determined by output noise measurement at short-circuit input termination $\left|\underline{Z}_{DUT}\right| \to 0$. Under this condition Eq. 10 simplifies into

$$S'_{in} = \frac{S_{i in}\cdot\left|R_{in}\right|^2 + S_{u in} + S_{u R_{in}}}{\left|R_{in} + Z_{fmil}\right|^2}. \quad (13)$$

In order to avoid possible saturation of SR570 due to input offset voltage, we have measured noise density spectra at

all transconductance settings at standard 50 Ω BNC input termination. Considering already determined parameters of noise sources, we extracted the input voltage noise from measurement. Each of two distinct spectra, shown in fig. 8, can be attributed to one of the two preamplifiers used for two transconductance ranges. They can also be modeled as a sum of flat and $1/f$ components , as shown in table 3.

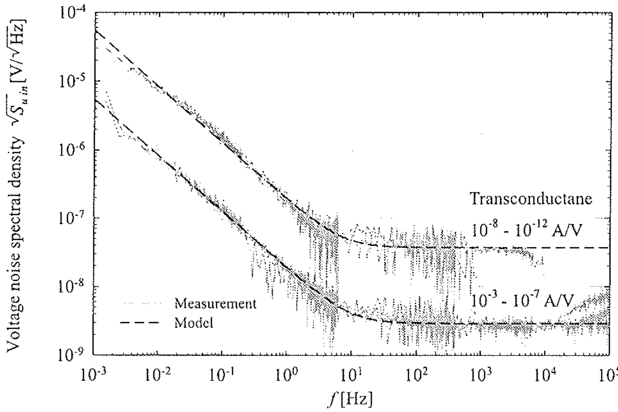

Fig. 8: Noise power density spectra of the equivalent input noise voltage source of SR570 at different sensitivities, extracted at 50 Ω input termination.

Table 3: The SR570 equivalent input noise voltage source parameters.

Transconductance range [A/V]	$S_{u\,in} = S_0 + A_f / f^{\gamma}$		
	$\sqrt{S_0}$ [V/√Hz]	$\sqrt{A_f}$ [V/√Hz]	γ
$10^{-3} \ldots 10^{-7}$	$2.9 \cdot 10^{-09}$	$1.9 \cdot 10^{-08}$	1.64
$10^{-8} \ldots 10^{-12}$	$3.5 \cdot 10^{-08}$	$1.7 \cdot 10^{-07}$	1.74

Using the obtained noise model we can investigate the influence of external factors to the overall noise of the SR570. The most direct one is the influence of the DUT impedance (Z_{DUT}), which will be shown separately for resistive and capacitive part, since most semiconductor photonic sensors exhibits capacitive nature. The influence of DUT resistance R_{DUT} on the system noise is presented for transconductance of 10^{-7} A/V in fig. 9. It is clearly seen, that the voltage noise increases while decreasing the R_{DUT} and would supersede other noise sources, if there wasn't input resistance R_{in}, which saturates the whole system noise. But unfortunately the current divider of R_{in} and R_{DUT} causes the decrease of the measured DUT current noise which further diminishes in the noise of R_{in}. Therefore for each transconductance setting there is a range of allowed DUT resistances that can give valid results. In the case of transconductance of 10^{-7} A/V this range spans approximately from 10^4 to 10^7 Ω.

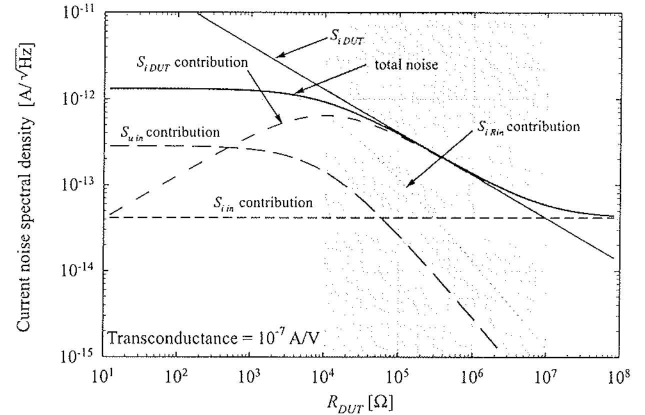

Fig. 9: Influence of the DUT resistance on the SR570 noise properties at f = 100 Hz. The usable R_{DUT} range is marked in gray.

To show the role of DUT capacitance (fig. 10) we chose the transconductance of 10^{-8} A/V, where the effect is more pronounced due to higher equivalent input noise voltage. At low frequencies the noise floor is limited by input current noise, while the influence of input voltage noise increases with frequency due to the decrease of DUT impedance. The DUT capacitance together with the inductive nature of input impedance forms a resonant peak, which can significantly raise the noise floor in case of high capacitive DUTs.

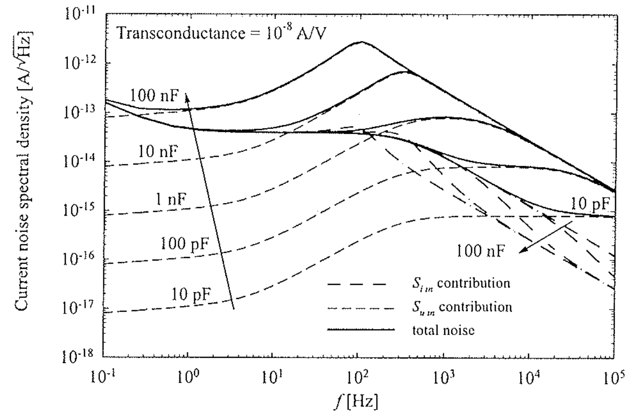

Fig. 10: Effect of the DUT capacitance on the SR570 noise performance.

3.3. Noise measurement of a-Si:H *pin* diode

In order to demonstrate the usefulness of the developed and characterized noise measurement setup results of noise measurement of an amorphous silicon (a-Si:H) *pin* diode are presented. The diode area was 1 mm^2 and the *p*, *i*, *n* layer thicknesses were 10, 400 and 20 nm, respectively. Since the noise model of our measurement system also requires known DUT impedance, we initially measured dynamic properties of the diode /9/.

From acquired system noise density spectra the part that originates from the diode is extracted using previously de-

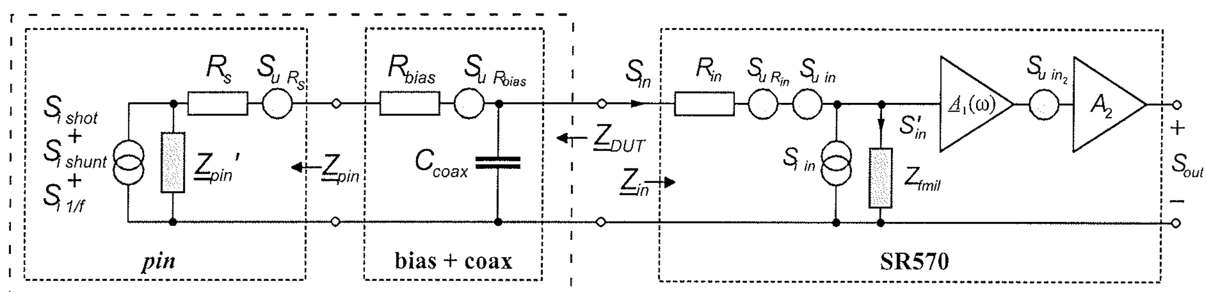

Fig. 11: Noise model of measurement system including a-Si:H pin diode, bias circuit, coaxial cable connection and SR570 transconductance amplifier.

scribed noise model of measurement system considering additional factors (voltage bias resistance thermal noise ($S_{u\,Rbias}$), coaxial cable capacitance C_{coax} and the noise model of the a-Si:H *pin* diode) as presented in fig. 11. The noise of offset voltage source U_{off} and the input noise of the SR780 FFT spectrum analyzer are neglected.

The noise model of the a-Si:H *pin* diode was formed on the basis of previously used noise models of similar devices /10, 11/. All dynamic parameters of the diode except series resistance R_s are combined in the impedance Z'_{pin}. The total noise of the a-Si:H *pin* diode is composed of three independent current noise sources: shot noise $S_{i\,shot}$, thermal noise of shunt resistance $S_{i\,shunt}$ and 1/*f* noise $S_{i\,1/f}$. In addition, a voltage thermal noise source of series resistance $S_{u\,Rs}$ is present. All noise sources except 1/*f* noise can be calculated from known diode parameters. The missing 1/*f* noise component is extracted from the measurement results accounting contributions of all other known noise components. Fig. 12 presents measured noise density spectra of aSi:H *pin* diode at forward bias of 420 nA at the output of SR570. Noise system components from noise model of the SR570 (Fig. 11) are shown as well. The influence of the voltage noise $S_{u\,in}$, particularly at lower frequencies, determines the system noise, which is a consequence of low diode impedance at forward bias. Measured noise spectrum prevails system noise almost in the whole frequency range and is approaching to the calculated noise spectrum of the measured diode at higher frequencies. The excess noise at frequencies below 100 Hz can be attributed to 1/*f* noise of the measured diode, but it diminishes in the system noise below 10 mHz, due to different slopes of spectra.

According to measured spectra, transferred to the input of SR570 (fig. 13), at frequencies above 100 Hz, shot noise of the diode ($S_{i\,shot}$) is dominant, while below 100 Hz the 1/*f* noise prevails. Thermal noises of series ($S_{u\,Rs}$) and shunt ($S_{i\,shunt}$) resistance are negligible. By subtracting the system, shot and thermal noise components from the measured noise, the excess noise spectrum can be extracted. It exhibits typical 1/*f* dependence and can be modeled by an empirical expression

$$S_{i,1/f} = \frac{A_f}{f^{\gamma}}, \qquad (14)$$

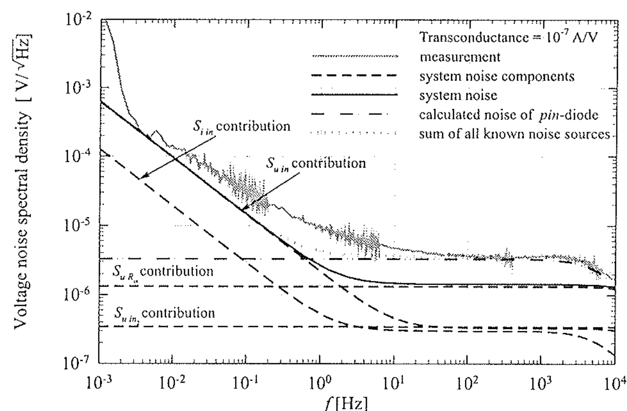

Fig. 12: Noise voltage density spectrum, measured at the SR570 output, of the a-Si:H pin diode at forward current bias of 420 nA. The contribution of individual noise sources of the measurement system and the known noise components of the pin diode are added for comparison. The observed excess noise is 1/f noise component of the pin diode.

where A_f is power density at f = 1 Hz and γ determines the slope of the spectrum. The 1/*f* shape of the spectrum with slope γ = 1.00 can be observed from f = 0.01 Hz (where it prevails system noise) up to 100 Hz, where it diminishes into the flat part of the spectrum. The noise current density of 1/*f* component at 1 Hz is $\sqrt{A_f} = 1.0 \cdot 10^{-12} \mathrm{A}/\sqrt{\mathrm{Hz}}$.

4. Discussion

The presented noise measurement system was successfully applied for the current noise measurement of a-Si:H *pin* diodes at low frequency range from 10 mHz up to 10 kHz. Below 10 mHz the high slope of the low-frequency system noise component makes the measurement uncertain, while the upper limit is determined mainly by the bandwidth of the LNA. One of the important outcomes of the presented study is that besides input current noise also input voltage noise of the transconductance amplifier is important. Its contribution is directly correlated to the impedance of the applied DUT, which also has to be known prior to actual noise measurement. In the case of low im-

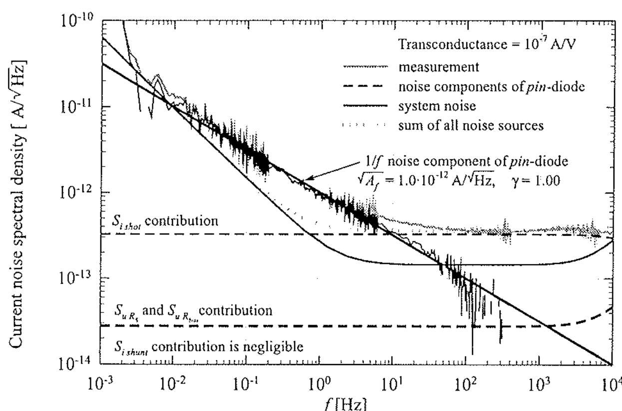

Fig. 13: Noise current density spectrum, transferred to the SR570 input, of the a-Si:H pin diode at forward current bias of 420 nA. The contribution of individual known noise sources of the pin diode and the total noise of the measurement system are added for comparison. The excess noise is subtracted from the calculated overall noise of the system, which yields 1/f noise component of the pin diode.

pedance or high capacitive DUTs the input voltage noise can mainly determine the total system noise performance. Thus, only by knowing all the parameters that influence the noise performance of the system, one can determine the part of the noise that originates from the DUT itself.

This is especially important in the case of noise measurements of high capacitive devices, such as large area aSi:H *pin* diodes with thin layers that exhibit high capacitance and very low intrinsic noise. In our case we could successfully measure only the smallest area diodes (1 mm^2) where the capacitance was sufficiently low thus keeping the input voltage noise below the critical values.

The problem of external low-frequency electric and magnetic interference was successfully eliminated by an arrangement of aluminum and mumetal shielding combination. The remaining external interference problems were mechanical vibrations that cause microphone effects in the input coaxial cable connections. This was partially solved by putting the system in the corner close to concrete walls and avoiding any movements near it as much as possible. Fortunately, the mechanical vibrations appear in the spectrum only at a certain frequencies and can be easily noticed. In such cases the measurement had to be repeated.

5. Conclusions

The low-frequency noise measurement system based on transconductance amplifier SR570 and a FFT spectrum analyzer SR780 was built. Dynamic and noise properties of the SR570 were thoroughly analyzed resulting in a comprehensive noise model of the complete measurement system. Besides other noise sources also 1/*f* noise components of the SR570 was identified. The influence of DUT impedance to the overall system noise properties was demonstrated. The noise measurement system utilizing the obtained noise model was used for low-frequency noise measurement of a-Si:H *pin* diodes. 1/*f* noise with the ideal slope (γ = 1.00) and noise density of $\sqrt{A_f} = 1.0\cdot10^{-12}\text{A}/\sqrt{\text{Hz}}$ at 1 Hz was identified to be dominant below 10 Hz, while above 10 Hz the diode's shot noise prevails.

6. References

/1/ E. Uiga, Optoelectronics, Prentice Hall, New Jersey, 1995, ISBN 0-02-422170-8.

/2/ Ambrozy, Electronic noise, Akademiai kiado, Budapest, 1982, ISBN 963 05 2665 4.

/3/ H. Yoshida, M. Yoshida, T. Shinoda, I. Saito, I/*f* noise produced by the random motion of the carriers crossing potential barriers in semiconductors, J. Appl. Phys., Vol. 76, No. 11, 1994, pp. 7372-7376.

/4/ F. Blecher, Noise of a-Si:H pin diode pixels in imagers at different operating conditions, MRS proc., vol. 557, 1999, pp. 869-874.

/5/ F. Blecher, Photo- and dark current noise in a-Si:H pin diodes at forward and reverse bias, MRS proc., Vol. 507, 1998, pp. 175-180.

/6/ P. A. W. E. Verleg, Fluctuationg defect density probed with noise spectroscopy in hydrogenated amorphous silicon, MRS proc., Vol. 467, 1997, pp. 221-225.

/7/ Model SR780 Network Signal Analyser Manual, Stanford Research Systems, 1996.

/8/ Model SR570 Low-noise Current Preamplifier, Stanford Research Systems, 2000.

/9/ H. Stiebig, U. Nosan, M. Krause, M. Jankovec, M. Topič, Dynamic properties of ultraviolet sensitive detectors, J. Non-Cryst. Solids 338-340, 2004, pp. 772-775.

/10/ R. Miller, Rauschen, Springer-Verlag, ISBN 3-540-51145-8, 1990.

/11/ M. Jankovec, H. Stiebig, F. Smole, M. Topic, Noise characterization of a-Si:H pin diodes, J. Non-Cryst. Sol. 352, 2006, pp. 1829-1831.

Dr. Marko Jankovec, univ. dipl. ing. el.
Prof. Dr. Marko Topič, univ. dipl. ing. el.

University of Ljubljana,
Faculty of Electrical Engineering
Laboratory of Photovoltaics and Optoelectronics
Tržaška cesta 25, SI-1000 Ljubljana, Slovenia
Tel.: +386 (0)1 4768 321
Fax:+386 (0)14264630
E-mail: marko.jankovec@fe.uni-lj.si

Prispelo (Arrived): 19.04.2007 *Sprejeto (Accepted):* 15.06.2007